AIAA Science and Technology Forum and Exposition, 23-27 January 2023, National Harbor, Maryland

A Computational Study of Plume Modeling For Space Launch System Abort Scenarios

Jonathan Boustani[1*], Michael P. Applebaum[1†], William M. Eppard[1‡],
Thomas B. Steva[2§], Leslie Hall[1¶]

[1]*CRM Solutions Inc. DBA Mclaurin Aerospace, Jacobs ESSCA Group, Huntsville, AL, 35802*

[2]*NASA Marshall Space Flight Center, Huntsville, AL 35808*

This extended abstract details work on Space Launch System (SLS) core stage drag during abort scenarios that is currently being conducted. In the final paper, viscous computational fluid dynamics simulations will be used to study the axial force coefficient on the SLS core stage as a function of its distance to the upstream crew module and launch abort system, the freestream conditions, and the chemical model used to represent the launch abort system abort motor and attitude control motor plumes. In addition, the computational expense of each method will be studied in order to help determine the appropriate trade-off between fidelity and simulation turn around time.

I. Introduction

During crewed missions of NASA's Space Launch System (SLS), astronauts will ride aboard the Orion Multi-Purpose Crew Vehicle (MPCV). In order to protect these astronauts during abort scenarios, the MPCV is shrouded by a launch abort system (LAS) containing three sets of solid rocket motors (SRM) along a tower atop the crew module.

During a pad or ascent abort scenario, an abort motor (AM) near the top of the LAS tower would fire for approximately three seconds, generating over 400,000 lbf of thrust, with the intention to quickly distance the crew in the MPCV from the core stage of SLS. One of the primary concerns during an ascent abort, however, is that the aborted core stage could catch up to and impact the MPCV. In fact, the presence of the MPCV and LAS disrupt the flow upstream of the aborted stack, lowering the axial force coefficient of the core stage. In these scenarios, the most conservative estimate of the axial force coefficient on the aborted core stage, CA, is 0, though this is an extremely limiting assumption. Instead, we propose the effect of the MPCV and LAS with the AM and attitude control motors (ACMs) firing on the axial force coefficient of the downstream aborted SLS Block 1 core stage be systematically studied with a series of viscous computational fluid dynamics (CFD) simulations.

The primary goals of this study are to determine: (1) the effect of the MPCV and LAS on the aerodynamic drag of the aborted core stage, and (2) the level of fidelity required to obtain conservative but efficient results. Goal (1) will be accomplished by varying the freestream conditions, the distance from the MPCV and LAS to the leading edge of the core stage, and the LAS AM thrust conditions while recording the change in axial force on the core stage. For Goal (2), a selected case will be run while modeling the AM and ACMs exhaust gases with an inert perfect air model, a chemically-perfect equivalent single-species model, a chemically-imperfect equivalent single-species model, and a true multispecies model including finite rate chemical kinetics and studying the effect of the modeling fidelity on the core stage drag. The exhaust gas models vary greatly in terms of computational cost, and if an acceptable, conservative answer can be found with significantly less

*Aerospace Engineer, jonathan.boustani@mclaurin.aero.
†Senior Aerospace Engineer
‡Senior Aerospace Engineer
§Aerodynamics Team Lead, Aerosciences Branch
¶Director of Engineering, AIAA Member

time and resources using one of these lower-fidelity approaches, its use may be justified in the mission design process.

II. Problem Description

The outer mold line (OML) used in the current work is derived from the SLS Block 1 crewed configuration. This is shown in Fig. 1. The MPCV and LAS are shown in grey, the relevant drag surfaces on the core stage and boosters are shown in blue, and the rest of the geometry is shown in orange. The geometry is placed in the center of a hemispherical domain, and an unstructured volume mesh is generated between the surface triangulation and the farfield (see Figs. 2) using Mississippi State's AFLR3.[?,?] This process yielded volume domains of approximately 270 million cells. All simulations are considered at an angle of-attack and side-sweep angle of 0°.

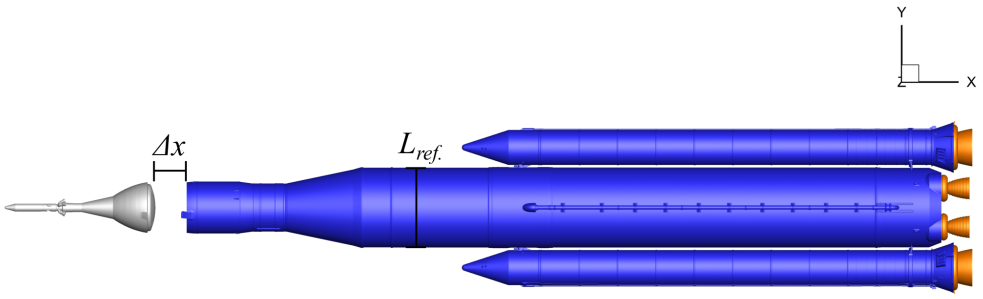


Figure 1: Schematic of the SLS Block 1 geometry used in the current work with the MPCV and LAS offset.

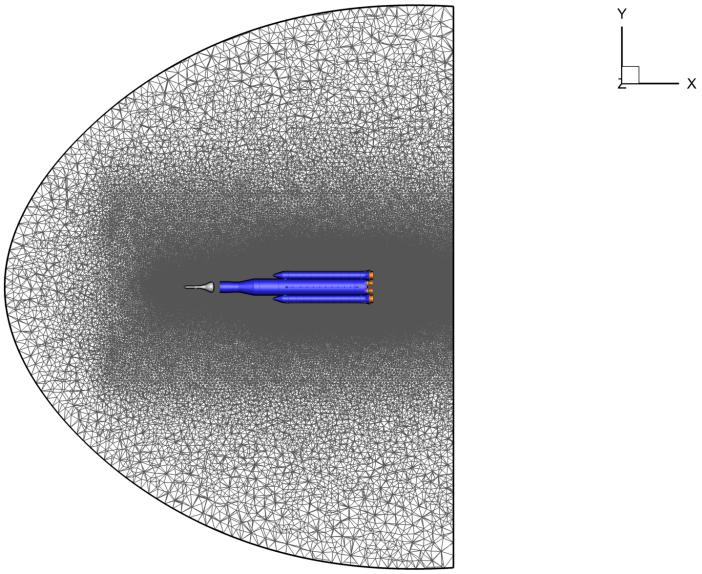


Figure 2: The unstructured volume mesh and domain boundaries shown on the $x-y$ plane.

In Fig. 1, a dimensional characteristic length of the SLS core stage was labeled as $L_{ref.}$, and the dimensional distance from the leading edge of the SLS core stage to the aft end of the MPCV was labled as Δx. In this work, the dimensionless MPCV/LAS offset, $\Delta x/L_{ref.}$, is varied from 0.5, 1.5, and 2.5 in order to determine a relationship between the offset distance and the core stage drag. In the final paper, the LAS AM thrust conditions will also be varied between relevant 'low-' and a 'high-thrust' condition, and the freestream Mach number will vary from $M = 0.7$ to $M = 3.0$ in order to consider the abort scenario at different altitudes. The full test matrix is summarized in Table 1.

Table 1: CFD Test Matrix

$\Delta x/L_{ref.}$	Mach Number	AM Thrust Level
0.5	0.7, 3.0	Low, High
1.5	3.0	Low, High
2.5	3.0	Low, High

III. Numerical Methods

All simulations were performed using steady-state time integration within Mississippi State's loci/CHEM viscous Navier-Stokes solver.[?,?] In order to handle the large discontinuities in the supersonic flow field, loci/CHEM's high-speed module is used. In this module, the convective terms are discretized with a blended Roe-HLLE scheme, the latter, more dissipative, scheme activating in and just downstream of regions with strong pressure gradients in the flow field. The solution of the highly-turbulent viscous terms is aided with Wilcox's $k-\omega$ model[?] and Wilcox's compressibility correction. All surfaces are treated as no-slip, adiabatic walls.

The ACM and AM exhaust gases are modeled with a 15-species, 30-reaction chemical kinetic model.[?] In the final paper, lower-fidelity models will be considered as well, and the effect of the other models on the core stage drag will be systematically studied.

IV. Preliminary Results

All cases detailed in Table 1 have been simulated, so far all with the fully-chemically reacting AM and ACM exhaust gas model. A correlation between the varying MPCV/LAS offset distance, freestream Mach number, and AM thrust levels and the axial force coefficient on the aborted core stage can then be formed, and in the final paper, the correlation will be reconstructed with the lower-fidelity exhaust gas models and compared.

A snapshot of the iteration-averaged pressure and temperature fields shown on a cut-plane through the center of two AM nozzles for the $\Delta x/L_{ref.} = 0.5$, low-thrust cases at $M = 0.7$ and $M = 3.0$ are shown in Figures 3a-3b and 3c-3d, respectively. The large differences in the subsonic and supersonic freestream conditions are evident by the drastically different flow features seen between the top and bottom rows of Fig. 3. In Fig. 3b, the higher ambient pressure and lower Mach number in the $M = 0.7$ case allow the plumes to continue normal to the exit plane of the nozzle far longer downstream while maintaining a fairly narrow profile. In Fig. 3d, however, the much lower ambient pressure allows the AM plumes to massively expand as they exit the nozzle, causing a portion of the plume to impinge on the leading surface of the LAS that shrouds the MPCV. The high-speed freestream keeps the AM plumes confined to a region near the body of the core stage, heating its surface significantly compared to Fig. 3b. The impingement of the high-temperature AM plumes on the MPCV and their subsequent confinement to a near-body region likely causes differences in the chemical composition of the gas mixture downstream of the leading edge of the core stage - something that will be studied further in the final paper.

The effect of the varying freestream conditions, and the AM thrust level, on the drag force and the axial force coefficient are now studied. Table 2 summarizes the effect of the freestream Mach number and AM thrust level on the axial force coefficient of the aborted core stage. All results are shown relative to the low-thrust, $M = 0.7$ case at $\Delta x/L_{ref.} = 0.5$. Given the same conditions, but considering a high AM thrust level, the second row of Table 2 indicates that the higher AM thrust is likely causing slightly wider and stronger plumes that shield the downstream aborted core stage from some of the oncoming dynamic pressure in the freestream. The AM thrust level seems to have less effect at the supersonic freestream conditions as is shown by the similar relative CA values for the last two cases in Table 2. This is likely due to the fact that the high-speed freestream and strong shocks forming on the launch vehicle stage adaptor and the forward attachment for the solid rocket boosters (SRBs) at this Mach number are dominating any secondary effects caused by the AM thrust level.

Interestingly, however, the massive change in freestream conditions and primary flow features between the $M = 0.7$ and $M = 3.0$ cases yields less than 0.5% change in the value of the axial force coefficient.

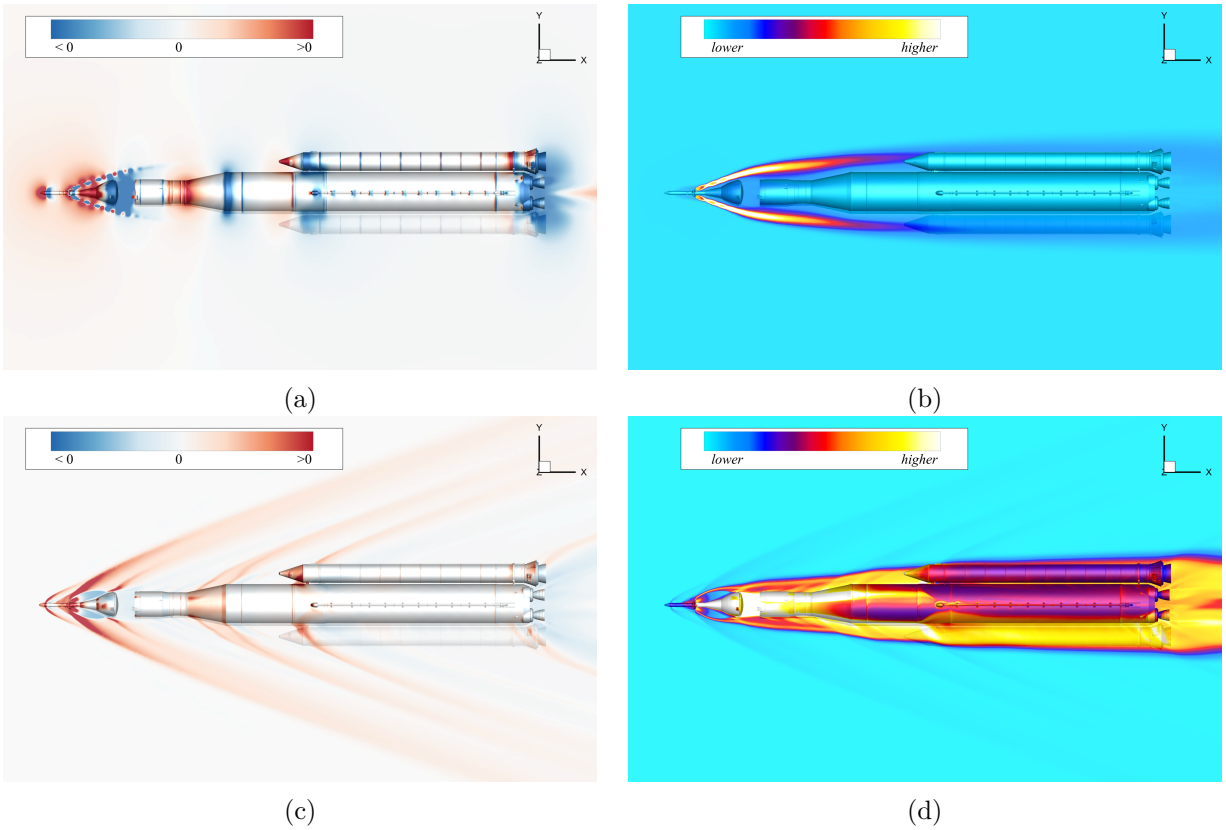


Figure 3: Saturated pseudocolor contours of iteration-averaged (left) pressure and (right) temperature for low-thrust, $\Delta x/L_{ref.} = 0.5$ simulations at (a)-(b) $M = 0.7$ and (c)-(d) $M = 3.0$ shown on a semi-transparent plane rotated through two AM nozzles and on the surface of the geometry.

Table 2: Summary of the Axial Force Coefficient as a Function of M and AM Thrust Level

$\Delta x/L_{ref.}$	Mach Number	AM Thrust Level	CA (relative)
0.5	0.7	Low	-
0.5	0.7	High	-2.83%
0.5	3.0	Low	+0.43%
0.5	3.0	High	+0.42%

While the dynamic pressures used at the two Mach numbers were similar, it could have been expected that additional wave drag from the shock structures may have increased CA in the $M = 3.0$ cases relative to the $M = 0.7$ cases more than they did. The possible cause of this, *e.g.*, a decrease in viscous forces at a higher Reynolds number, a decrease in inviscid forces due to a deficit in dynamic pressure on the core stage caused by 'shielding' from shocks forming on the MPCV/LAS, or something more nuanced (chemical reactions) will be studied thoroughly in the final paper.

The final item that will be studied in this extended abstract is that of the axial force coefficient as a function of the MPCV/LAS offset distance. So far, a value of $\Delta x/L_{ref.} = 0.5$ has been considered, which will now be varied to 1.5 and 2.5 for the $M = 3.0$ cases only. Snapshots of iteration-averaged density contours can be seen for each offset distance in Fig. 4. The effect of the MPCV and LAS on the flow field upstream of the aborted core stage is most clearly seen here. In Figs. 4a and 4b, the MPCV and LAS are sufficiently 'shielding' the core stage behind the strong bow shocks forming just upstream of the ACMs and AMs. By Fig. 4c, however, the MPCV is sufficiently far away from the core stage to allow the beginnings of a bow

shock to form on its leading edge. In fact, a wake is allowed to form behind the heat shield of the MPCV, as shown by the characteristic recompression shock in Fig. 4c halfway between the MPCV and core stage. This wake interferes with the development of the bow shock ahead of the cavity at the leading edge of the core stage, but the bow shock is allowed to form some radial distance off the of the core stage. It can then be expected that large pressures form on the leading edge of the core stage as the MPCV moves upstream, and we are likely to see a positive correlation between $\Delta x/L_{ref.}$ and the axial force coefficient on the core stage.

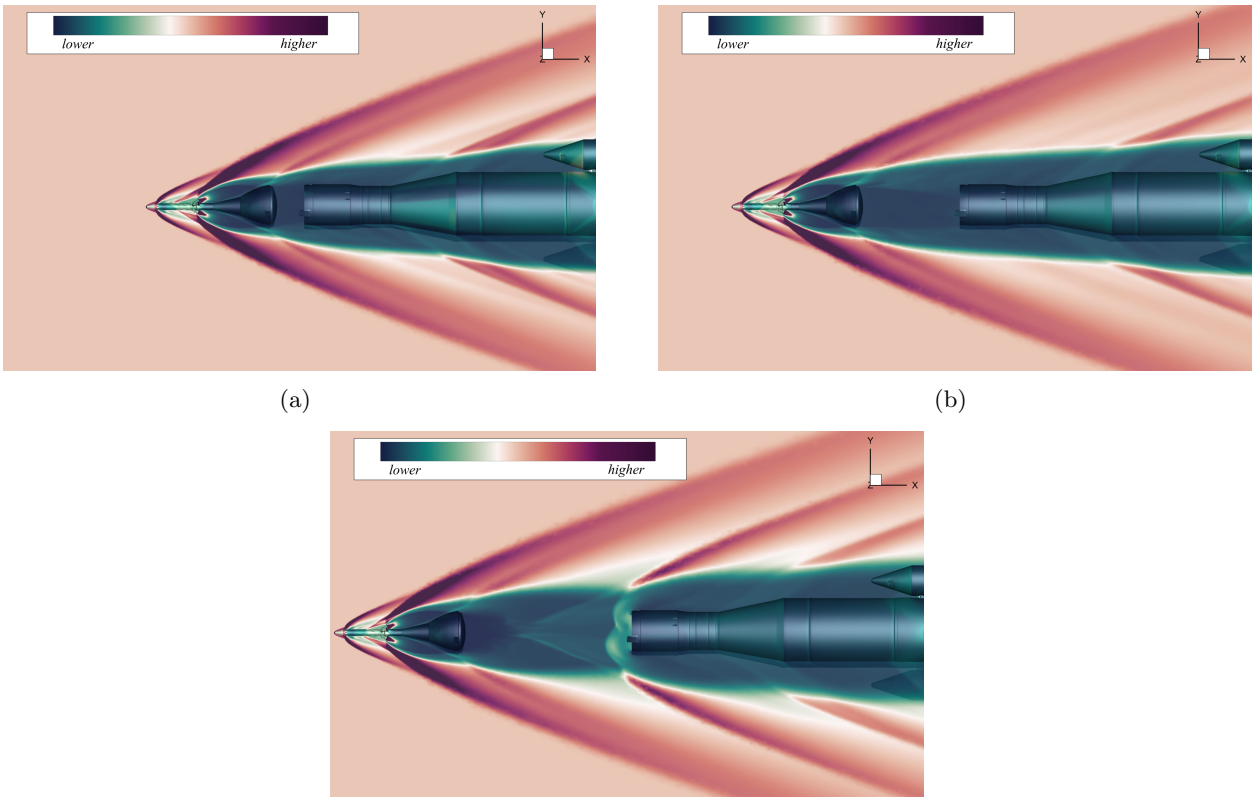


Figure 4: Saturated pseudocolor contours of the iteration-averaged density for low-thrust, $M = 3.0$ simulations at $\Delta x/L_{ref.}$ = (a) 0.5, (b) 1.5, and (c) 2.5 shown on a semi-transparent plane rotated through two AM nozzles and on the surface of the geometry.

The results of this study are summarized in Table 3, where CA is shown as a function of $\Delta x/L_{ref.}$. Compared to $\Delta x/L_{ref.} = 0.5$, at $\Delta x/L_{ref.} = 1.5$, approximately a 10% increase in CA is observed as 'shielding' from the MPCV/LAS decreases. By $\Delta x/L_{ref.} = 2.5$ however, CA nearly doubles in value. This is for the reasons made clear in the previous paragraph, that the flow is allowed to form a bow shock ahead of the aborted core stage. This causes a significant increase in drag on the core stage.

Table 3: Summary of the Axial Force Coefficient as a Function of $\Delta x/L_{ref.}$

$\Delta x/L_{ref.}$	Mach Number	AM Thrust Level	CA (relative)
0.5	3.0	Low	-
1.5	3.0	Low	+10.2%
2.5	3.0	Low	+92.4%

So far neglected has been an extended analysis on the fidelity of the chemical model used for the ACM and AM exhaust gases, and its effect on the core stage drag as a evaluated function of the variables studied

in this extended abstract. That is, we have not answered whether an equivalent species model, or even a perfect air model, can predict the core stage drag sufficiently close to the values predicted by the fully chemically reacting model. Furthermore, those findings would then need to be tested as functions of the freestream Mach number, AM thrust level, and MPCV/LAS offset distance. It may be the case that at sufficiently large offset distances, the plumes have time and space to cool before reaching the core stage, thus affecting the chemical composition of the mixture in the near body region and possibly the drag on the core stage, rendering a chemically-perfect equivalent species or inert air model less useful. All of these items will be studied in detail in the final paper.

V. Conclusions

In this extended abstract, the problem of possible core stage recontact with the MPCV during abort scenarios was detailed, and a solution involving a series of viscous CFD simulations was presented. loci/CHEM's viscous Navier-Stokes solver was used to simulate the SLS Block 1 configuration during different abort scenarios using a true multispecies model with chemical kinetics to model the ACM and AM exhaust gases. Plans for the final paper, considering less-expensive, but less accurate, chemical models were also discussed.

In the preliminary simulations with the fully reacting chemical model, it was found that the freestream dynamic pressure and AM thrust level, while having large effects on the topology of the AM plumes, had little effect of the drag of the aborted core stage. This is an interesting finding that will be thoroughly investigated in the final paper. Finally, it was shown that the factor with the largest influence on the core stage drag was the distance of the MPCV and LAS from the leading edge of the aborted core stage. In fact, at a sufficiently far distance upstream, the drag predicted on the core stage nearly doubled. This was attributed to the MPCV and LAS having less effect on the flow field in the region immediately upstream of the core stage.

The final paper will reconsider these findings using chemical models with less fidelity and studying the effect of the presence of the plumes and even the MPCV and LAS it self on the prediction of drag on the aborted core stage. The ultimate goal is to provide the agency with conservative estimates of the core stage drag during abort scenarios with a quick enough turn around time and a reasonable amount of computational resources such that hundreds, possibly thousands, of simulations can be conducted that fully define the drag of the core stage as a function of many factors.